
Article:
Zhang, Y., Scarratt, N.W., Wang, T. et al. (1 more author) (2016) Fabricating high performance conventional and inverted polymer solar cells by spray coating in air. Vacuum. ISSN 0042-207X

https://doi.org/10.1016/j.vacuum.2016.09.017

Fabricating high performance conventional and inverted polymer solar cells by spray coating in air

Yiwei Zhang[1], Nicholas W. Scarratt[1†], Tao Wang[2*], David G. Lidzey[1*]

[1]Department of Physics and Astronomy, University of Sheffield, Sheffield, S3 7RH, UK

*E-mail: twang@whut.edu.cn ; d.g.lidzey@sheffield.ac.uk

[†] Current address: Ossila Ltd, Kroto Innovation Centre, Broad Lane, Sheffield, S3 7HQ, UK.

Abstract: We report bulk heterojunction organic solar cells utilising the electron-donating polymer PffBT4T-2OD blended with the fullerene acceptor $PC_{71}BM$, with cells explored based on both conventional and inverted architectures. As charge-transporting layers, we utilise the hole-transporting polymer poly (2, 3-dihydrothieno-1, 4-dioxin)-poly (styrenesulfonate) **(**PEDOT:PSS) in conventional device architectures, and zinc oxide (ZnO) electron-transport in inverted devices. Critically, all charge-transporting layers and the poly[(5,6-difluoro-2,1,3-benzothiadiazol-4,7-diyl)-alt- (3,3000-di(2-octyldodecyl) 2,2'; 50,2''; 500,2000 -quaterthiophen-5,5000-diyl)] (PffBT4T-2OD): [6,6]-phenyl C71 butyric acid methyl ester ($PC_{71}BM$) active layer blend were spray coated in air. We demonstrate champion devices having a power conversion efficiency of 8.13% and 8.43% for conventional and inverted architectures respectively.

Keywords: Spray-casting, bulk heterojunction solar cells, OPV, PEDOT:PSS, ZnO, PffBT4T-2OD:$PC_{71}BM$

Highlights:

- PEDOT:PSS, ZnO precursor and PffBT4T-2OD:$PC_{71}BM$ films were fabricated into organic photovoltaic (OPV) devices, with all layers spray coated in air.
- The Power Conversion Efficiency (PCE) of OPV devices utilising a PEDOT:PSS hole transport layer and PffBT4T-2OD:$PC_{71}BM$ active-layer was 8.13%.
- The PCE of OPV devices utilising the ZnO electron transport layer and PffBT4T-2OD:$PC_{71}BM$ active-layer was 8.43%.

Organic photovoltaic devices (OPVs) represent a promising technology to convert solar energy to electricity, and can in principle be fabricated at low-cost on large area and flexible substrates. [1-5] In the past decade, the performance of OPVs has improved dramatically as a result of the development of new organic semiconductors and innovative processes for manufacture. Best devices now have a power conversion efficiency (PCE) exceeding 10%; [6, 7] a value that has been considered as a milestone in the commercialisation of OPVs.[8] In order to advance the development of OPVs, it is still necessary to explore new, efficient semiconducting materials, together with innovative ways to fabricate devices.

Recently, a polymer namely poly[(5,6-difluoro-2,1,3-benzothiadiazol-4,7-diyl)-alt-(3,3'''-di(2-octyldodecyl) 2,2';5',2'';5'',2'''-quaterthiophen-5,5'''-diyl)] (PffBT4T-2OD) has been synthesised and has attracted much interest.[9, 10] When processed appropriately, PffBT4T-2OD:$PC_{71}BM$ blend films exhibit high crystallinity, high hole mobility and can form polymer domains having high purity; a combination of factors that allow this material to work in an efficient manner in an OPV device even when it is presented as a relatively thick layer (up to 300 nm). Using this material, OPVs have now been reported having a PCE up to 10.8%.[10] Although the efficiency is one of the highest yet reported for a polymer-based device, the conditions used in thin-film deposition and device fabrication can influence the degree of polymer aggregation and crystallisation and thus can significantly affect device performance.[9] We note that the polymer PffBT4T-2OD has a tendency to aggregate in solution; a property that presents a significant obstacle during device fabrication.

Most reports of OPV fabrication using PffBT4T-2OD:$PC_{71}BM$ rely on the use of spin coating under a nitrogen atmosphere. Spin coating however cannot be used in a high volume fabrication

process, and critically it is a wasteful process that requires the use of relatively high concentration solutions resulting in problems due to aggregation and loss of expensive material. In contrast, spray coating has been used in the fabrication of OPVs and is compatible with large area processing over flexible substrates.[11-15] Notably, most work on the development of spray cast OPVs have explored blend of the polymer poly (3-hexylthiophene) (P3HT) and (6, 6)-phenyl-C61 butyric acid methyl ester (PCBM). These materials are seen as being a prototypical OPV system, but are limited by relatively low PCE.[16] More recent work has however explored spray-cast blends of amorphous donor-acceptor co-polymers with fullerene-derivative electron acceptors, with improved device performance demonstrated. [11, 13, 17, 18]

Spray-coating has also been used to deposit the various charge transporting layers used in OPV devices. [19] In single junction OPV device based on a conventional architecture, the active layer is deposited onto a hole-transporting layer. Here, a widely used material is the polymer PEDOT:PSS which can be spray-cast from an aqueous solution in air[12]. In so-called inverted devices, the active-layer blend is instead deposited on an electron-transporting layer such as zinc oxide (ZnO). Here, ZnO can be easily processed from solution using a sol-gel method, [20, 21] with such materials also being compatible with deposition by spray coating.[14, 22] We note that inverted devices can have significant advantages resulting from higher efficiencies and improved operational stability.[23, 24]

In this study, we fabricate PffBT4T:2OD:$PC_{71}BM$ based bulk heterojunction OPVs based on both conventional and inverted architectures. Here, the PffBT4T:2OD:$PC_{71}BM$ active layer, the PEDOT:PSS hole transport layer (HTL) and the ZnO electron transport layer (ETL) are all spray coated in air. By optimising the composition of the PffBT4T:2OD:$PC_{71}BM$ ink, conventional and

inverted architecture OPVs were fabricated having champion efficiencies of 8.13% and 8.43% respectively.

The device architectures investigated in this work, together with the chemical structure of PffBT4T-2OD and $PC_{71}BM$ materials is shown in Figure 1. Spray coating was conducted using a Prism 300 ultra-sonic spray coater (Ultrasonic Systems Inc.) that was operated in air under regular clean-room conditions. This spray coater is a nozzle-less system, with the ultrasonic vibrating spray tip enabling the generation of a fine droplet mist; a crucial element in the creation of high-quality, uniform films.[25] To fabricate devices, our processes started with (20mm x 15mm) glass substrates coated with pre-patterned ITO electrodes (purchased from Ossila Ltd). Before use, the substrates were sequentially cleaned using an ultra-sonic bath containing Hellmanex solution, 2-propanol (IPA) and deionised water.

To prepare PEDOT:PSS ink for spray coating, PEDOT:PSS (Heraeus Clevios P VP AI 4083) was filtered through a 0.45μm filter and then mixed with IPA and ethylene glycol (EG) according to a volume ratio of 1:8:1. Here, IPA and EG were used to tune the wetting property and viscosity of the ink to form a uniform film on the surface of the ITO.[12] During spray coating, the substrates were heated to 30°C to facilitate the formation of a uniform film. During coating, a tip-substrate distance of 70 mm was maintained, with a lateral tip velocity of 80 mm/s used to create a film having a thickness of approximately 30 nm. The films deposited were then immediately annealed at 120°C for 5 minutes before being ready for use.

The precursor gel used to fabricate the ZnO ETL was prepared by dissolving 110 mg zinc acetate dihydrate in 1ml 2-methoxyethanol with 30μl ethanolamine as stabiliser. The solution was then stirred for 12 hours in air to form a transparent gel. Before spray coating, the resultant gel was

diluted using methanol at a volume ratio of 1:8 to reduce its viscosity. For spray-coating, a tip-substrate distance was maintained at 45 mm, with a lateral tip velocity of 25 mm/s used to prepare films having a thickness of 25 nm. Here, films were sprayed onto substrates held at room temperature. The films were then annealed at 275ºC for 5 minutes to convert the precursor film to zinc oxide.

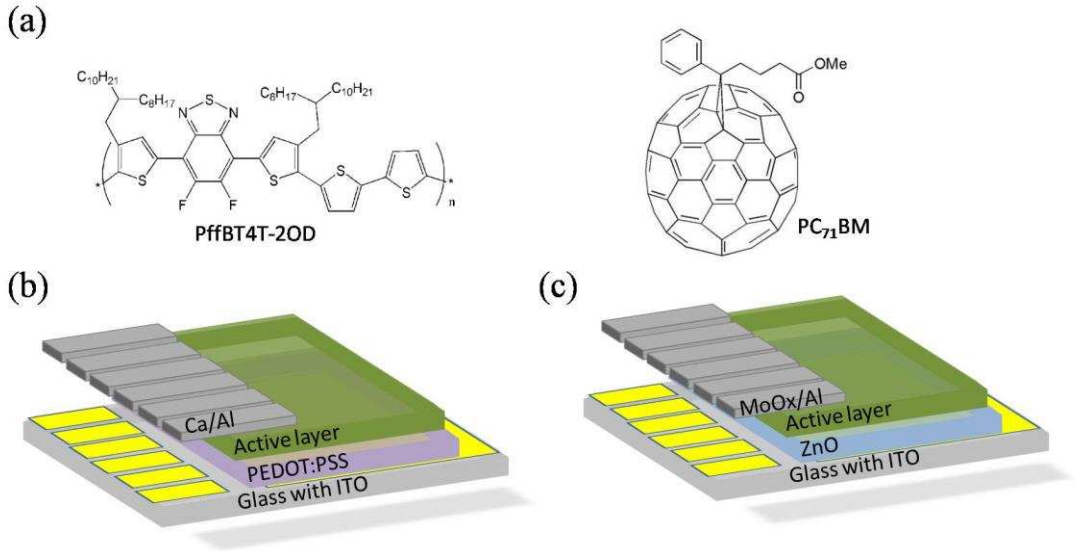

Figure 1: (a) Molecular structure of PffBT4T-2OD and $PC_{71}BM$. Part (b) shows a conventional device, while part (c) shows an inverted OPV architecture.

We have used an atomic force microscope (AFM) to evaluate the surface roughness of spray coated PEDOT:PSS and ZnO films as shown in Figure 2. Here, parts (a) and (b) show spin- and spray-cast PEDOT:PSS, parts (c) and (d) shown spin- and spray-cast ZnO, whilst parts (e) and (f) show a spin- and spray cast PffBT4T-2OD:$PC_{71}BM$ blend. In these experiments, the films were spin / spray-cast onto a blank glass substrate.

We have used these images to assess the relative roughness of the films, and to compare films that have been spin- and spray cast. Comparing images (a) and (b) we determine a quadratic mean roughness (RMS) of spin-coated and spray-cast PEDOT:PSS to be 1.41 and 1.96 nm respectively.

From images (c) and (d), we similarly find spin- and spray-cast ZnO have an RMS roughness of 1.16 and 1.35 nm respectively. We find therefore that the spray-cast charge extraction layers are in both cases slightly rougher than their spin-cast analogues, however we have previously found that such values are not detrimental OPV performance. [13]

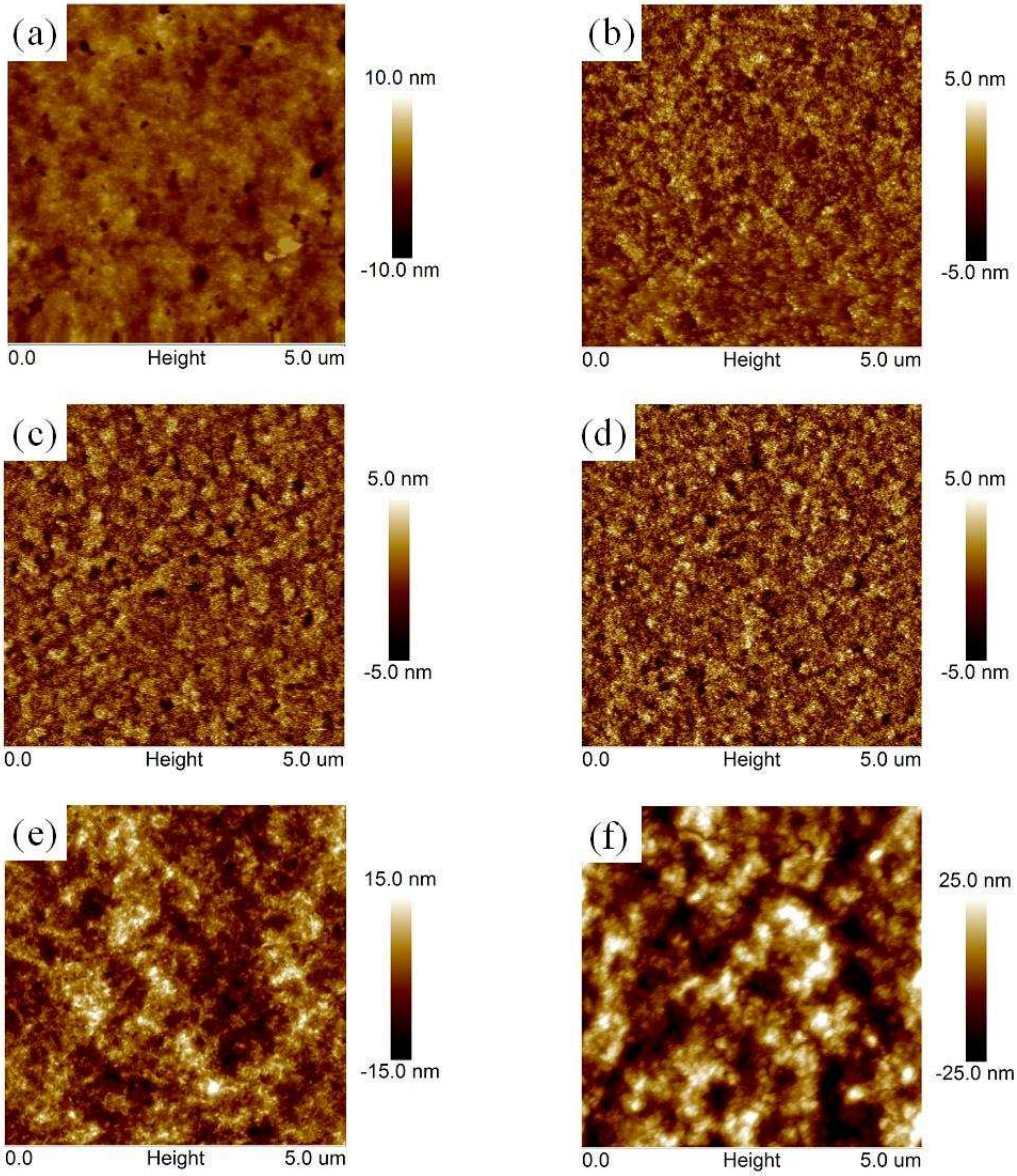

Figure 2: AFM surface morphology of (a) spin coated PEDOT:PSS and (b) spray coated PEDOT:PSS. Parts (c) and (d) show surface morphology of spin coated and spray coated ZnO respectively. In parts (e) and (f) we similarly show images of spin-coated and spray-cast PffBT4T-2OD:$PC_{71}BM$ blend films.

To coat the active layer, we prepared an ink consisting of 1:1.2 weight ratio of PffBT4T-2OD:$PC_{71}BM$ dissolved at 5 mg/ml into a mixture of the solvents chlorobenzene (CB) and 1,2-dichlorobenzene (DCB) (volume ratio 1:1). The solvent mixture also contained a small (3%) volume concentration of 1,8-diiodooctane (DIO) in order to optimise the micro nanostructure of the BHJ film.[26, 27] Before use, the ink was stirred at 110ºC for 5 hours to ensure the solids in the blend were fully solubilised. Notably, the relatively low concentration of solids used in this ink (formulated for spray-coating) effectively suppresses aggregation problems of PffBT4T-2OD that often occur in higher concentration solutions that have been optimized for spin-coating. The active PffBT4T-2OD:$PC_{71}BM$ layer was then spray-cast onto the substrates held at 85°C. It was found that this substrate temperature encouraged the formation of a uniform film. Through extensive optimization spray trials, we determined that a spray tip velocity of 25mm/s at a tip-substrate separation of 45 mm created films having a thickness 250 nm.

A typical AFM image of spin-cast and spray-cast PffBT4T-2OD:$PC_{71}BM$ blend films is shown in Figures 2 (e) and (f) respectively. It can be seen that the spray-cast films is slightly rougher than the spin coated one (RMS of 4.65 nm compared to 7.32 nm respectively), however, in such thick films, the bulk morphology may well determine device performance, with the morphology of the surface playing a secondary role.

OPV devices were then fabricated by transferring the spray-coated films to a nitrogen filled glove box. They were then left for 3 hours under nitrogen to dry, after which were placed in a vacuum vessel at $5x10^{-6}$ mbar for a further hour to remove all casting solvent (especially the DIO). Films were then transferred onto a hot-plate in the glove box and annealed at 100°C for 5 minutes to complete the drying process. It was found that this final anneal process was important in

optimising device performance. Then top electrode was then thermal evaporated onto the active layer through a shadow mask under a vacuum of $2x10^{-6}$ mbar. Here, conventional architecture devices employed a top (electron extracting) cathode consisting of 5 nm calcium (Ca) and 100 nm aluminium (Al). For inverted architecture devices, the top anode instead consisted of a 10 nm molybdenum oxide (MoO_x) film capped by 100 nm of Al (with all films deposited by thermal evaporation). Finally, devices were encapsulated using UV cured epoxy glue and a glass cover slip.

To test the photovoltaic properties, JV curves were recorded while the devices were illuminated using a Newport 92251A-1000 AM 1.5 solar simulator calibrated against an NREL standard silicon solar cell. In all cases, an aperture mask was placed on top of the device to ensure the light-exposed area of the device was limited to $2.6mm^2$.

We plot champion device data in Figure 3 and summarise key metrics in Table 1. Specifically, 'champion' conventional devices reached an efficiency of 8.13%. For inverted devices, a champion efficiency of 8.43% was obtained. For completeness, Figure 3 and Table 1 also includes device metrics and JV curves for nominally identical devices in which both charge transport layers were spin coated in air, with the photo-active layers instead spin coated in a nitrogen filled glove box. It can be seen the efficiency of the spin-coated devices are higher than equivalent devices fabricated by spray coating, with PCEs of 9.02% and 9.36% determined for conventional and inverted devices respectively. This loss in efficiency primarily results from a reduction in Jsc, which suggest that the slight loss of performance on spray-coating most probably results from photo-oxidation of the active layer as it was exposed to the atmosphere. [28, 29] We note that some high-performing OPV polymers can be very sensitive to exposure to light in the presence of

oxygen,[11] whilst others are apparently significantly more stable. [30] We believe that such oxidation could be reduced by performing air-based spray-coating of the active layer under appropriate safe-lights.

To illustrate the repeatability of these measurements, we summarise the distribution of PCE recorded from 32 pixels distributed over 8 different substrates for both conventional and inverted devices in Figures 3(c) and (d). In these measurements, we excluded data recorded from the two edge pixels in our analysis, as the film quality at the edge of the substrate often suffers from poor uniformity resulting in poor device performance. It can be seen the repeatability of the spray coated devices (both conventional and inverted structure) is promising. Although the area of the substrates used in this work is limited, our work highlights the possibility to fabricate high performance OPV devices based on highly crystalline polymers via spray coating.

Table 1: Key metrics for conventional and inverted devices fabricated by spin- and spray-coating.

Device	PCE(%)	V_{oc}(V)	J_{sc}(mA/cm^2)	FF(%)
Spin-coated conventional	9.02 (8.70±0.15)	0.76 (0.75±0.01)	-17.55 (-16.88±0.40)	67.96 (68.37±0.83)
Spray-coated conventional	8.13 (7.13±0.44)	0.75 (0.74±0.01)	-16.47 (-14.28±0.91)	65.88 (67.19±2.49)
Spin-coated inverted	9.36 (9.11±0.26)	0.75 (0.75±0.01)	-17.68 (-17.24±0.84)	70.33 (70.19±1.71)
Spray-coated inverted	8.43 (7.75±0.46)	0.75 (0.74±0.01)	-16.08 (-15.64±0.63)	70.19 (66.73±1.92)

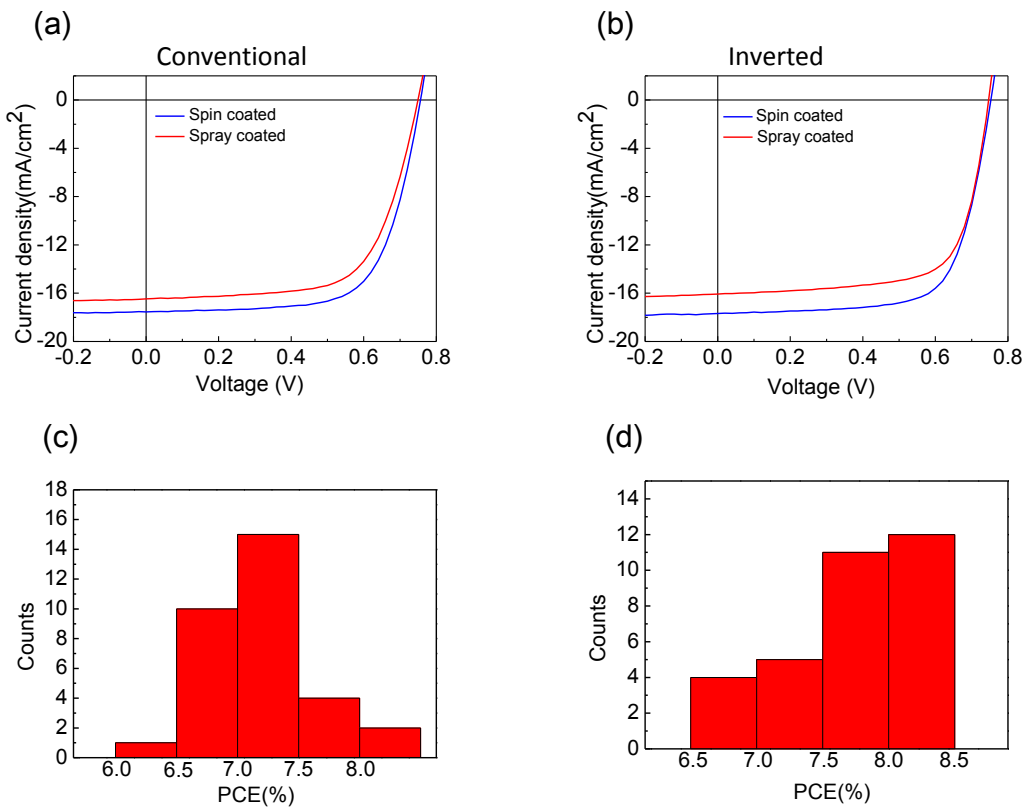

Figure 3: Part (a) and (b) shows J-V curves of champion conventional and inverted devices fabricated by spin- and spray- coating. Pats (c) and (d) show a distribution of device PCE recorded from spray-coated conventional and inverted devices respectively.

In summary we have investigated the performance of conventional OPVs incorporating spray coated PEDOT:PSS hole transport layer and PffBT4T-2OD:$PC_{71}BM$ photoactive layers. This has been compared with inverted OPVs based on a spray coated ZnO electron transport layer and a PffBT4T-2OD:$PC_{71}BM$ photoactive layer. Critically the photoactive ink is based on the highly crystalline polymer PffBT4T-2OD that can be spray coated from cold solution without obvious problems resulting from aggregation. We determine a PCE of 8.13% for conventional devices and 8.43% for inverted devices using a gentle post deposition thermal annealing process which most likely removes any trapped casting solvent. Our work further demonstrates the feasibility of

fabricating high performance OPVs via spray coating.

Acknowledgement

We thank financial support from EPSRC via grants EP/I028641/1 “Polymer/fullerene photovoltaic devices: new materials and innovative processes for high-volume manufacture”, EP/J017361/1 “Supergen Supersolar Hub” and EP/M025020/1 “High resolution mapping of performance and degradation mechanisms in printable photovoltaic devices”. T.W. acknowledges funding support from the National Natural Science Foundation of China (Grant No. 21504065). Y.Z. thanks the University of Sheffield for providing a PhD scholarship.

References

[1] Scharber M, Sariciftci N. Efficiency of Bulk-Heterojunction Organic Solar Cells. Progress in Polymer Science. 2013;38:1929-40.
[2] Dou L, You J, Hong Z, Xu Z, Li G, Street RA, et al. 25th Anniversary Article: A Decade of Organic/Polymeric Photovoltaic Research. Adv Mater. 2013;25:6642-71.
[3] Li G, Zhu R, Yang Y. Polymer solar cells. Nat Photonics. 2012;6:153-61.
[4] Darling SB, You F. The case for organic photovoltaics. Rsc Adv. 2013;3:17633-48.
[5] Wang T, Pearson AJ, Lidzey DG. Correlating molecular morphology with optoelectronic function in solar cells based on low band-gap copolymer: fullerene blends. Journal of Materials Chemistry C. 2013;1:7266-93.
[6] Green MA, Emery K, Hishikawa Y, Warta W, Dunlop ED. Solar cell efficiency tables (Version 45). Progress in Photovoltaics: Research and Applications. 2015;23:1-9.
[7] Chen JD, Cui C, Li YQ, Zhou L, Ou QD, Li C, et al. Single-Junction Polymer Solar Cells Exceeding 10% Power Conversion Efficiency. Adv Mater. 2014;27:1035-41.
[8] Sheats JR. Manufacturing and commercialization issues in organic electronics. J Mater Res. 2004;19:1974-89.
[9] Ma W, Yang G, Jiang K, Carpenter JH, Wu Y, Meng X, et al. Influence of Processing Parameters and Molecular Weight on the Morphology and Properties of High-Performance PffBT4T-2OD:PC71BM Organic Solar Cells. Adv Energy Mater. 2015;5:1501400.
[10] Liu Y, Zhao J, Li Z, Mu C, Ma W, Hu H, et al. Aggregation and morphology control enables multiple cases of high-efficiency polymer solar cells. Nat Commun. 2014;5:5293.
[11] Zhang Y, Griffin J, Scarratt NW, Wang T, Lidzey DG. High efficiency arrays of polymer solar cells fabricated by spray-coating in air. Progress in Photovoltaics: Research and Applications.

2016;24:275-82.
[12] Scarratt NW, Griffin J, Wang T, Zhang Y, Yi H, Iraqi A, et al. Polymer-based solar cells having an active area of 1.6 cm2 fabricated via spray coating. APL Mater. 2015;3:126108.
[13] Wang T, Scarratt NW, Yi HA, Dunbar ADF, Pearson AJ, Watters DC, et al. Fabricating High Performance, DonorAcceptor Copolymer Solar Cells by Spray-Coating in Air. Adv Energy Mater. 2013;3:505-12.
[14] Kang J-W, Kang Y-J, Jung S, Song M, Kim D-G, Su Kim C, et al. Fully spray-coated inverted organic solar cells. Sol Energ Mat Sol C. 2012;103:76-9.
[15] Girotto C, Moia D, Rand BP, Heremans P. High-Performance Organic Solar Cells with Spray-Coated Hole-Transport and Active Layers. Adv Funct Mater. 2011;21:64-72.
[16] Susanna G, Salamandra L, Brown TM, Di Carlo A, Brunetti F, Reale A. Airbrush spray-coating of polymer bulk-heterojunction solar cells. Sol Energ Mat Sol C. 2011;95:1775-8.
[17] Reale A, La Notte L, Salamandra L, Polino G, Susanna G, Brown TM, et al. Spray Coating for Polymer Solar Cells: An Up-to-Date Overview. Energy Technol-Ger. 2015;3:385-406.
[18] Kannappan S, Palanisamy K, Tatsugi J, Shin P-K, Ochiai S. Fabrication and characterizations of PCDTBT: PC71BM bulk heterojunction solar cell using air brush coating method. J Mater Sci. 2012;48:2308-17.
[19] Griffin J, Pearson AJ, Scarratt NW, Wang T, Lidzey DG, Buckley AR. Organic photovoltaic devices incorporating a molybdenum oxide hole-extraction layer deposited by spray-coating from an ammonium molybdate tetrahydrate precursor. Org Electron. 2014;15:692-700.
[20] Sun YM, Seo JH, Takacs CJ, Seifter J, Heeger AJ. Inverted Polymer Solar Cells Integrated with a Low-Temperature-Annealed Sol-Gel-Derived ZnO Film as an Electron Transport Layer. Adv Mater. 2011;23:1679.
[21] Yang T, Cai W, Qin D, Wang E, Lan L, Gong X, et al. Solution-Processed Zinc Oxide Thin Film as a Buffer Layer for Polymer Solar Cells with an Inverted Device Structure. The Journal of Physical Chemistry C. 2010;114:6849-53.
[22] Kang Y-J, Lim K, Jung S, Kim D-G, Kim J-K, Kim C-S, et al. Spray-coated ZnO electron transport layer for air-stable inverted organic solar cells. Sol Energ Mat Sol C. 2012;96:137-40.
[23] Norrman K, Madsen MV, Gevorgyan SA, Krebs FC. Degradation Patterns in Water and Oxygen of an Inverted Polymer Solar Cell. J Am Chem Soc. 2010;132:16883-92.
[24] Jorgensen M, Norrman K, Gevorgyan SA, Tromholt T, Andreasen B, Krebs FC. Stability of Polymer Solar Cells. Adv Mater. 2012;24:580-612.
[25] Barrows AT, Pearson AJ, Kwak CK, Dunbar ADF, Buckley AR, Lidzey DG. Efficient planar heterojunction mixed-halide perovskite solar cells deposited via spray-deposition. Energ Environ Sci. 2014.
[26] Lou SJ, Szarko JM, Xu T, Yu L, Marks TJ, Chen LX. Effects of Additives on the Morphology of Solution Phase Aggregates Formed by Active Layer Components of High-Efficiency Organic Solar Cells. J Am Chem Soc. 2011;133:20661-3.
[27] Chen Y, Zhang X, Zhan C, Yao J. Origin of Effects of Additive Solvent on Film-Morphology in Solution-Processed Nonfullerene Solar Cells. Acs Appl Mater Inter. 2015;7:6462-71.
[28] Soon YW, Cho H, Low J, Bronstein H, McCulloch I, Durrant JR. Correlating triplet yield, singlet oxygen generation and photochemical stability in polymer/fullerene blend films. Chem Commun. 2013;49:1291-3.
[29] Huang W, Gann E, Xu Z-Q, Thomsen L, Cheng Y-B, McNeill CR. A facile approach to alleviate

photochemical degradation in high efficiency polymer solar cells. J Mater Chem A. 2015;3:16313-9.
[30] Bovill E, Yi H, Iraqi A, Lidzey DG. The fabrication of polyfluorene and polycarbazole-based photovoltaic devices using an air-stable process route. Appl Phys Lett. 2014;105:223302.